Systematic model behavior of adsorption on flat surfaces

R. A. Trasca, M. W. Cole, and R. D. Diehl

Department of Physics, The Pennsylvania State University, University Park, Pennsylvania 16802, USA
(Received 5 June 2003; published 10 October 2003)

A low density film on a flat surface is described by an expansion involving the first four virial coefficients. The first coefficient (alone) yields the Henry's law regime, while the next three terms in the expansion correct for the effects of adsorbate-adsorbate interactions, computed within the two-dimensional approximation (a film confined nearly to a plane). The results permit exploration of the idea of universal adsorption behavior, which is compared with experimental data for a number of systems. The idea works well, in general, justifying a general model of adsorption at low to moderate coverage.

I. INTRODUCTION

Nearly half a century ago the first adsorption experiments were carried out that yielded behavior interpreted in terms of two-dimensional (2D) theoretical models [1]. The agreement with those models was a consequence of the fact that high surface area forms of graphite present extended, uniform, and flat areas, as is assumed in the models. Subsequently, a wide variety of techniques have found similar behavior on other surfaces [2]. With an abundance of such data comes the opportunity to address questions about universality of the behavior. If universal relations are appropriate, it facilitates the planning and interpretation of new experiments.

In this paper, we address this question and several others. To be specific, we examine the nature of low coverage adsorption, using the technique of the virial expansion. In this case, the expansion includes both gas-surface and gas-gas interactions. Fortunately, virial coefficients incorporating the interparticle interactions are available, facilitating this work. Hence, the principal effort reported here involves using these coefficients along with a simple description of the motion perpendicular to the surface. The results include numerical values of the pressure threshold for adsorption and the relationship between the isosteric heat of adsorption and the well depth of the gas-surface interaction. In addition, the validity of the expansion is tested by comparing the predictions with experimental data for diverse adsorption systems.

II. DESCRIPTION OF THE MODEL

The simplest model of a monolayer film in coexistence with vapor considers it as a classical noninteracting gas in an external field, the interaction with the substrate [2]. Assuming that the adsorbate atoms move freely across the surface, the potential energy of adsorption is a function of the normal coordinate z alone. An accurate representation of many adsorption potentials, sufficient to describe the energetics and dynamics in the vicinity of the minimum [3], is

$$V(z) = -D + \kappa(z - z_0)^2/2, \tag{1}$$

where κ is the force constant, D is the well depth, and the equilibrium position is z_0. The solution for the number density of a noninteracting gas in the potential $V(z)$ follows as

$$n(z) = n(\infty)\exp[-\beta V(z)], \tag{2}$$

where $\beta = 1/(k_B T)$, T is the temperature, and $n(\infty)$ is the vapor density as $z \rightarrow \infty$, where the true potential energy [but not Eq. (1)] vanishes. Then, the film coverage on a surface of area A is given by the expression [4]

$$N = A \int n(z)dz = n(\infty) \int \exp[-\beta V(z)]dz. \tag{3}$$

With the assumed quadratic dependence of V on z and the equation for an ideal gas $n(\infty) = \beta P$, the film's two-dimensional density $\theta = N/A$ is given by

$$\theta = \beta P \sqrt{\left(\frac{2\pi}{\beta\kappa}\right)} \exp(\beta D). \tag{4}$$

This Arrhenius form is the generic behavior of adsorption isotherms, with an activation energy equal to the well depth. Thus, thermodynamic techniques can be employed for finding the pressure-temperature conditions necessary for adsorption and probe the well depth [5,6]. However, the non-interacting gas model is applicable only at very low densities.

An improved model should take into account interactions between the adsorbate atoms, the effect of which usually predominates over effects of quantum statistics (except at very low temperatures for light and weakly interacting gases) [7–11]. This improvement is provided by the virial expansion, a series expansion whose leading term denotes the ideal-system results, while subsequent terms provide corrections arising from the interparticle interactions. For an isoenergetic, or structureless, substrate for which the motion is well confined to the plane $z = 0$, the problem becomes essentially 2D. The virial expansion of the equation of state of a two-dimensional gas can be written in the form [12]

$$\beta\Pi = \theta + B_{2D}\theta^2 + C_{2D}\theta^3 + D_{2D}\theta^4 + \cdots, \tag{5}$$

where Π is the 2D (spreading) pressure of the monolayer film. B_{2D}, C_{2D}, and D_{2D} are the 2D second, third, and fourth virial coefficients, respectively. In the 2D case, assumed here, the second virial coefficient is related to the two-body interaction through the equation
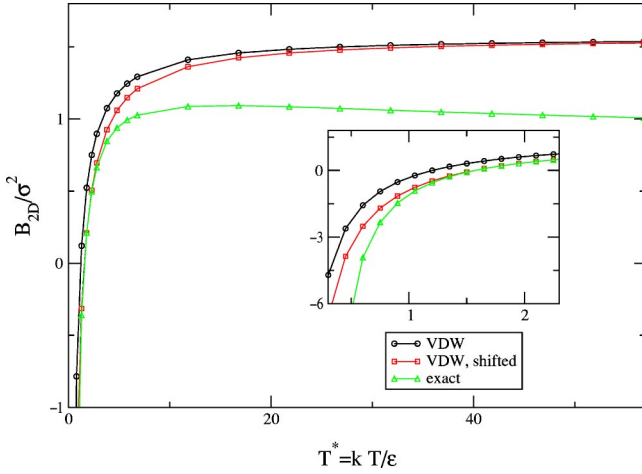
FIG. 1. (Color online) The reduced second virial coefficient as a function of reduced temperature. The triangles correspond to an exact calculation [Eq. (6)], the circles use the VDW approximation [Eq. (9)], and the square curve is obtained by shifting the VDW curve to the right (corresponding to an increase in gas well depth: $\epsilon_{VDW}=1.3\epsilon$). Inset shows low T behavior.

$$B_{2D}=-\pi\int_0^\infty dr\, r\{\exp[-\beta u(r)]-1\}, \qquad (6)$$

where r is the intermolecular separation and $u(r)$ is the pair potential. The van der Waals (VDW) theory is sometimes used to find an approximation of the second virial coefficient

$$B_{2D}^{VdW}\approx 1/2\int_0^\sigma d^2r+\beta/2\int_\sigma^\infty u(r)d^2r. \qquad (7)$$

In the case of a Lennard-Jones-type of interaction

$$u(r)=4\epsilon\left[\left(\frac{\sigma}{r}\right)^{12}-\left(\frac{\sigma}{r}\right)^{6}\right], \qquad (8)$$

where ϵ and σ are the interparticle well depth and hard-core diameter, respectively. Using this interaction, the second virial coefficient in the VDW approximation is

$$B_{2D}^{VdW}=\frac{\pi\sigma^2}{2}-\beta\frac{3\pi\epsilon\sigma^2}{5}. \qquad (9)$$

We computed both the "real" B_{2D} and its VDW approximation, as indicated in Fig. 1. Note that they differ appreciably at any T. However, one can shift the VDW approximation by adjusting the parameters a and b in the equation $B_{2D}=b-\beta a$. The adjustment to a and b was done by modifying the interparticle well depth to $\epsilon_{VDW}=1.3\epsilon$, a correction which improves the accuracy of the VDW approximation as seen in the figure. In this way, we got a good fit to B_{2D} at intermediate T, corresponding to the range of many experiments. At very high T, however, both VDW curves converge to a finite value, while the real B_{2D} goes to zero.

The third virial coefficient is related to the two-body interactions in clusters of three particles and is defined by the equation (in the 2D approximation)

$$C_{2D}=-\frac{1}{3}\int_0^\infty dr_2 dr_3\{\exp[-\beta u(r_{12})]-1\}\{\exp[-\beta u(r_{13})]$$

$$-1\}\{\exp[-\beta u(r_{23})]-1\}. \qquad (10)$$

This expression omits any explicit three-body interactions [13]. Details of the computation and tables of numerical values of B_{2D} and C_{2D} can be found in the original sources [10,12].

The equation of state relates the spreading pressure Π to θ and T. However, in an experiment one usually manipulates P and T. Therefore, we seek a relationship $P(\theta,T)$. This can be accomplished by employing the equilibrium condition between the gas phase and the adsorbed film,

$$\mu_{gas}=\mu_{film}, \qquad (11)$$

where μ is the chemical potential in the respective phase. The chemical potential of the gas (assumed ideal and spinless) phase is well known to be

$$\beta\mu_{gas}=\ln(\beta P\lambda^3), \qquad (12)$$

where

$$\lambda=\frac{h}{(2\pi mkT)^{1/2}} \qquad (13)$$

is the thermal wavelength of the particles. A derivation of μ_{film} appears in the Appendix, together with a discussion of the limitations of this approach:

$$\beta\mu_{film}=\ln(\theta\lambda^2)-\beta D+2B_{2D}\theta+\tfrac{3}{2}C_{2D}\theta^2+\tfrac{4}{3}D_{2D}\theta^3. \qquad (14)$$

Using the equilibrium condition [Eq. (11)], the relationship between θ, P, and T is found

$$\theta=\beta P\lambda\,\exp(\beta D)\exp(-2B_{2D}\theta-\tfrac{3}{2}C_{2D}\theta^2-\tfrac{4}{3}D_{2D}\theta^3). \qquad (15)$$

A kind of universal version of this equation appears if the thermodynamic quantities are replaced with reduced (dimensionless) quantities. Thus, P can be written as a function of a dimensionless pressure (P^*): $P=P^*\epsilon/\sigma^3$. In the same way, $D=D^*\epsilon$, $k_BT=T^*\epsilon$, and $\theta=\theta^*/\sigma^2$. The virial coefficients can also be reduced as $B_{2D}^*=B_{2D}/\sigma^2$, $C_{2D}^*=C_{2D}/\sigma^4$, and $D_{2D}^*=D_{2D}/\sigma^6$. A comparison of Eqs. 15 and 4 puts λ in correspondence with $\sqrt{2\pi/\beta\kappa}$, which will be used instead of λ. The force constant κ is taken to be D/σ^2, which is consistent with the universality of potentials, discussed in Ref. [3]. These simplifications result in a universal adsorption equation

$$\theta^*=P^*\sqrt{\frac{2\pi}{T^*D^*}}\exp(D^*/T^*)$$

$$\times\exp\left(-2B_{2D}^*\theta^*-\frac{3}{2}C_{2D}^*\theta^{*2}-\frac{4}{3}D_{2D}^*\theta^{*3}\right). \qquad (16)$$
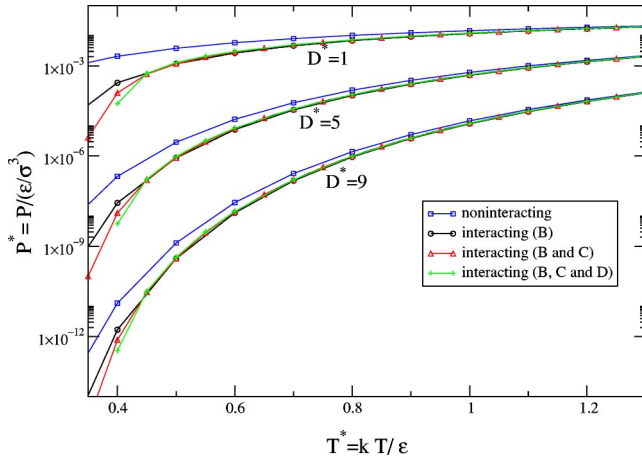
FIG. 2. (Color online) Reduced pressure at threshold for adsorption as a function of reduced temperature for three reduced well-depth values D^*. The squares correspond to a noninteracting gas, the circles take into account interactions through B_{2D}, the triangles include both B_{2D} and C_{2D}, and the plus curves include the fourth virial term. In each case, little or no adsorption occurs below the curve.

An important question (particularly useful for planning experiments) we address is this: What value of P^* produces "significant" adsorption? By significant, we mean the opposite of non-negligible, arbitrarily defined as reduced density $\theta^* \geqslant 0.1$. Below this density, the virial expansion should suffice over much of the relevant range of T, so we employ it to determine this pressure threshold. Figure 2 shows the resulting adsorption threshold curves for various numbers of virial terms and for three different values of D^*. Note that (for a specific well depth) the four curves converge at high T, since then the effect of gas-gas interactions disappears. At intermediate T, in contrast, the effect of interactions is to enhance the adsorption, which begins at a lower reduced pressure. The limitations of the virial expansion approach is seen in the difference between the curves with and without C. At low T, the curves diverge and the C_{2D} correction is large, as is that of D_{2D} (for $T^* < 0.45$). Thus, we conclude that higher-order corrections cannot improve the convergence of the virial series, since the virial coefficients are themselves divergent for $T^* < 0.45$ [12,10,14]. This divergence is consistent with the 2D critical temperature of different gases ($T_c^* \simeq 0.5$) [15].

The curves presented in Fig. 2 can be applied to treat specific adsorbates and substrates. The standard LJ parameters are well known in the literature [11,16]. However, when comparing our results with experiments, we assessed effects of the reduction of LJ well depth due to substrate screening effects (the McLachlan interaction) [17,18]. Table I presents both sets of parameters.

Adsorption experiments allow one to find the isosteric heat, which is a rough measure of the gas-substrate well depth. The relationship between the isosteric heat and well depth is not straightforward. The isosteric heat is

$$Q_{st} = -\left(\frac{\partial \ln P}{\partial \beta}\right)_N. \quad (17)$$

TABLE I. Standard and screened LJ parameters. Notice the well depth (ϵ) reduction due to screening [17,18] when adsorbed on graphite and Ag(111). The change of σ due to screening is not significant, thus is not shown.

Gas	$\epsilon_{standard}$ (K)	$\epsilon_{screened}^{Gr}$ (K)	$\epsilon_{screened}^{Ag}$ (K)	σ_{st} (Å)
Xe	221	214	185	4.10
Kr	171	150	135	3.60
Ar	120	110	96.7	3.40
H_2	37.0	27.3		3.05
Ne	35.6	33.8		2.75
N_2	36.4			3.32
CO	49.6			3.14
CH_4	148			3.45
He	10.2			2.56

The adsorption equation [Eq. (15)] allows us to find the P-T relation, from which one obtains

$$\beta Q_{st} = \frac{1}{2} + \beta D - 2\theta \frac{dB_{2D}}{d\ln\beta} - \frac{3\theta^2}{2}\frac{dC_{2D}}{d\ln\beta}. \quad (18)$$

In dimensionless form

$$Q_{st}^* - D^* = \frac{1}{2}T^* + 2(T^*)^2 \frac{dB_{2D}^*}{dT^*}\theta^* + \frac{3}{2}(T^*)^2 \frac{dC_{2D}^*}{dT^*}(\theta^*)^2, \quad (19)$$

where $Q_{st}^* = Q_{st}/\epsilon$ is the reduced isosteric heat. Figure 3 shows the difference between the reduced isosteric heat and the well depth, as a function of T in three cases: noninteracting gas, interacting gas including only B_{2D}, and interacting gas including both B_{2D} and C_{2D}. For specificity, we consider the case of $\theta^* = 0.1$. Let us focus first at low T: the difference between Q_{st}^* and D^* is small for the noninteracting model (T^*), but for the interacting gas the isosteric heat and well depth differ more due to the (overall attractive)
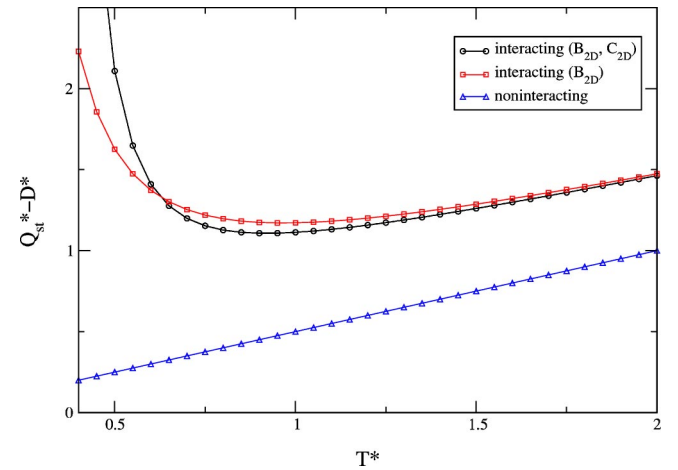

FIG. 3. (Color online) Difference between the reduced isosteric heat and the well depth as a function of reduced temperature in three cases at $\theta^* = 0.1$: noninteracting gas (triangle), interacting gas through B_{2D} (square), and interacting gas with B_{2D} and C_{2D} (circle).

gas-gas interactions. (Again, caution must be applied with the derivatives of virial coefficients, divergent for $T \lesssim 0.5$.) For intermediate values of T^*, this difference is of the order of the well depth ϵ, which is particularly important in cases when $\epsilon \gtrsim D$. At $T^* \approx 2$, the interacting and noninteracting models yield quite different values of Q_{st}. This can be seen easily for the second coefficient, computed in the VDW approximation,

$$(T^*)^2 \frac{dB^*_{VDW}}{dT^*} = \frac{3\pi}{5}. \tag{20}$$

When $T \rightarrow \infty$, however, B_{VDW} is still finite while $B_{2D} \rightarrow 0$. Thus, the noninteracting and interacting models converge at high T to the limit $Q^*_{st} - D^* = T^*/2$.

III. COMPARISON WITH EXPERIMENTS

A relevant assessment of these expressions is possible for adsorption on graphite and Ag (111) substrates, since there is a large body of experimental data for these surfaces. The data were obtained from electron diffraction studies of the adsorption of various gases. During these experiments, gas was adsorbed under quasiequilibrium conditions and the intensity of the diffraction spots from the substrate was measured. The attenuation of these diffraction beams provides a measure of the amount of gas adsorbed; in all of these cases, distinct "steps" were observed in the resulting equilibrium isobars or isotherms, corresponding to adsorption of the first layer. (Subsequent steps corresponding to subsequent layers were also observed in most cases, but those are not relevant to this paper.) By studying this behavior over a range of pressure or temperature, it is possible to produce an "isostere" curve in the P-T plane for any chosen coverage. The coverages chosen in the experimental studies cited here were the half-monolayer and monolayer coverages. Because of the limitation posed by the mean free path of electrons, gas pressures higher than about 10^{-3} mbar were inaccessible in these experiments, and therefore the range of data available for comparison is the pressure range between about 10^{-11} mbar and 10^{-3} mbar.

As sources for our well depth values, we used Ref. [19] for graphite and Ref. [20] for Ag(111). Results of our calculations are shown (using the screened LJ parameters from Table I) in Fig. 4 (for graphite) and Fig. 5 [for Ag(111)]. The experimental data were taken from various references [21–30]. The calculated curves are in overall good agreement with the experimental points, taking into account the approximations we made to achieve a simple, universal curve. However, we noticed that the calculations are sensitive to the gas interaction parameters; the standard LJ parameters yield lesser agreement than those of the screened interaction. The discrepancies between the calculated curves and some data points may be due to the fact that our calculations are performed at coverages much lower than a monolayer, while experiments usually tabulate the pressure and temperature values related to the completion of the monolayer. However, experimentally, the low coverage pressure (at the onset of adsorption) does not usually differ appreciably from the
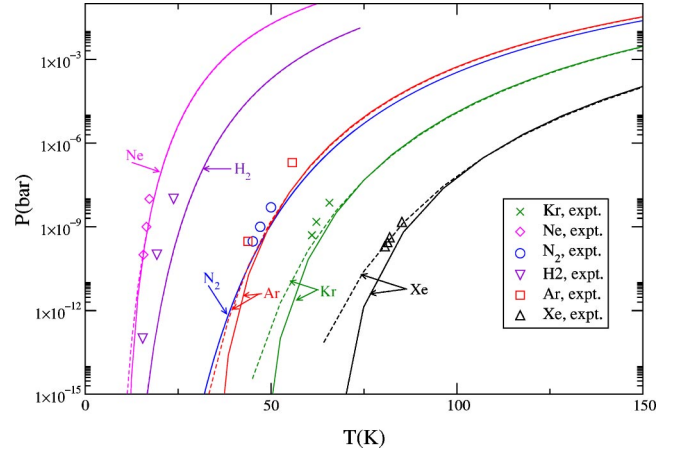

FIG. 4. (Color online) Threshold pressure of various gases on graphite compared with various experiments discussed in the text. The dashed curves take into account B_{2D} and the full curves include both B_{2D} and C_{2D}.

monolayer completion pressure. As mentioned above, the virial expansion is not convergent for $T < 0.4\epsilon$; therefore for gases with large ϵ, some experimental points may be in this range and thus other theoretical methods (Monte Carlo simulations) should be applied.

IV. CONCLUSIONS

Virial expansion calculations were performed in order to find the pressure-temperature threshold of adsorption on various surfaces assumed to be atomically smooth and perfect so they conform to the 2D approximation. Employing the equilibrium condition between the film and vapor, an equation relating P to θ and T was found and reduced to a universal equation. A comparison between the noninteracting and interacting models showed that the effect of interactions is to enhance the onset of adsorption, which occurs at lower pressure than in the noninteracting case. At high T, there is
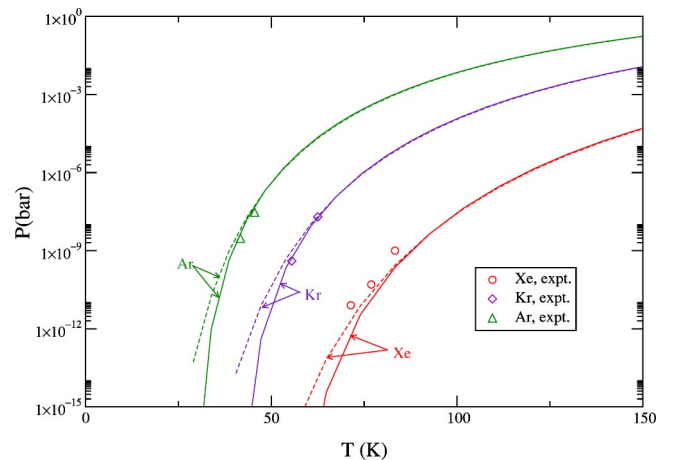

FIG. 5. (Color online) Threshold pressure of various gases on Ag(111) compared with various experiments discussed in the text. The dashed curves take into account B_{2D} and the full curves include both B_{2D} and C_{2D}.

little difference between the noninteracting and interacting curves, while at intermediate T, the difference between them is larger. At very low T, the virial coefficients are divergent. The computed threshold of adsorption was tested for various gases adsorbed on graphite and Ag(111). The calculated curves are in good agreement with the experimental ones. However, some of the experimental points lie in a range where the virial expansion diverges, so the comparison is incomplete. Finally, we addressed the relationship between the isosteric heat and the well depth. Due to interactions, these quantities differ appreciably at low T, while at high T the noninteracting and interacting cases converge to the same values.

ACKNOWLEDGMENTS

APPENDIX

The film's chemical potential can be found from the thermodynamic equation

$$\beta\mu_{film} = -\left(\frac{\delta\ln Q_N}{\delta N}\right)_T, \tag{A1}$$

where Q_N is the N-particle partition function of the film. The partition function for a noninteracting 2D gas can be factorized into Q_{2D}, associated with motion parallel to the surface, and Q_z, associated with motion perpendicular to the surface. Then, the partition function can be written as

$$Q_N = \frac{1}{N!}\left(\frac{A}{\lambda^2}Q_z\right)^N, \tag{A2}$$

where A is the area of the film. The molecules' motion perpendicular to the surface depends on the gas-surface interaction potential, here taken as $V(z) = -D + \kappa z^2/2$. Then, the quantum partition function for the z motion is

$$Q_z^{quan} = \sum_{n=0}^{\infty}\exp\{-\beta[-D+\hbar\omega(n+1/2)]\}$$

$$= \frac{\exp[\beta(D-\hbar\omega/2)]}{1-\exp(-\beta\hbar\omega)} = \frac{\exp(\beta E_b)}{1-\exp(-\beta\hbar\omega)}. \tag{A3}$$

Here, $\hbar\omega/2$ is the zero point energy, $1-\exp(-\beta\hbar\omega)$ comes from excitations to higher levels, and $E_b = D - \hbar\omega/2$ is the binding energy. Classically, instead

$$Q_z^{cl} = \int\frac{dz}{\lambda}\exp[-\beta(-D+\kappa z^2/2)] = \frac{\exp(\beta D)}{\beta\hbar\omega}. \tag{A4}$$

Thus, the ratio of Q_z^{cl} to Q_z^{quan}

$$R = \frac{Q_z^{cl}}{Q_z^{quan}} = \frac{2\sinh(\beta\hbar\omega/2)}{(\beta\hbar\omega)}. \tag{A5}$$

A high T expansion yields $R \approx 1 + (\beta\hbar\omega)^2/24$. This expansion works well up to $\beta\hbar\omega = 1$, at which point $R = 1.04$. At $\beta\hbar\omega = 1.5$, $R = 1.1$. Since one takes the logarithm to get the chemical potential, a 10% difference in Q_z is not significant. For the high T regime, $\beta\hbar\omega < 1.5$. Therefore the classical approximation can be used for most purposes, and it yields

$$\beta\mu_{film} = \ln(\theta\lambda^2) - \beta D + \ln(\beta\hbar\omega). \tag{A6}$$

For $\beta\hbar\omega$ of order 1, the last term in the above equation is negligible, and it makes only logarithmic corrections elsewhere. Thus, the film chemical potential at low density is essentially

$$\beta\mu_{film} \simeq \ln(\theta_0\lambda^2) - \beta D, \tag{A7}$$

where $\theta_0 = N/A$ is the film coverage at low densities. In deducing this equation the film was supposed to be a 2D noninteracting gas. The calculation of the chemical potential, including interactions through the fourth virial coefficient, can be found with the 2D Gibbs-Duhem equation

$$\left(\frac{\partial\mu}{\partial\Pi}\right)_T = \frac{1}{\theta}. \tag{A8}$$

Integrating

$$\left(\frac{\partial\mu}{\partial\theta}\right)_T = \left(\frac{\partial\mu}{\partial\Pi}\right)_T\left(\frac{\partial\Pi}{\partial\theta}\right)_T$$

$$\simeq (1 + 2B_{2D}\theta + 3C_{2D}\theta^2 + 4D_{2D}\theta^3)/(\theta\beta) \tag{A9}$$

from a very low density θ_0 (where the gas can be considered noninteracting) to a higher density θ, the film chemical potential becomes

$$\beta\mu_{film} = \ln(\theta\lambda^2) - \beta D + 2B_{2D}\theta + \tfrac{3}{2}C_{2D}\theta^2 + \tfrac{4}{3}D_{2D}\theta^3. \tag{A10}$$

---

[1] W.A. Steele, *The Interaction of Gases with Solid Surfaces* (Pergamon, Oxford, 1974).

[2] L.W. Bruch, M.W. Cole, and E. Zaremba, *Physical Adsorption: Forces and Phenomena* (Oxford University Press, Oxford, 1997).

[3] As discussed in G. Ihm, M.W. Cole, F. Toigo, and G. Scoles, J. Chem. Phys. **87**, 3995 (1987), physisorption exhibits a universal reduced potential form, with a force constant essentially $(D^5/C_3^2)^{1/3}$, where C_3 is the van der Waals coefficient and D is

the well depth. Using this force constant, one can deduce the adsorbate's vibrational displacement at any temperature; if it is larger than the characteristic length $(C_3/D)^{1/3}$, the assumed quadratic form is not adequate.

[4] For the present paper, we do not distinguish between the film coverage and the thermodynamic excess coverage, obtained by subtracting from Eq. (3) the integral in the case $V=0$; the latter requires a specification of the film domain, which is ambiguous.

[5] E.R. Conrad and M.B. Webb, Surf. Sci. **129**, 37 (1983).

[6] W.E. Packard and M.B. Webb, Surf. Sci. **195**, 371 (1988).

[7] Z.C. Guo and L.W. Bruch, J. Chem. Phys. **77**, 1417 (1982).

[8] R.L. Siddon and M. Schick, Phys. Rev. A **9**, 907 (1974).

[9] R.K. Pathria, *Statistical Mechanics* (Oxford University Press, Oxford, 1999).

[10] W.A. Steele, Surf. Sci. **39**, 149 (1973).

[11] M.J. Bojan and W.A. Steele, Langmuir **3**, 116 (1987); **3**, 1123 (1987).

[12] I.D. Morrison and Sydney Ross, Surf. Sci. **39**, 21 (1973).

[13] C.G. Gray and K.E. Gubbins, *Theory of Molecular Fluids* (Clarendon Press, Oxford, 1984), Vol. 1, Chap. 3.6.

[14] E.D. Glandt, J. Chem. Phys. **68**, 2952 (1978).

[15] See Ref. [2], p.122.

[16] R.O. Watts and I.J. McGee, *Liquid State Chemical Physics* (Wiley, New York, 1976).

[17] S. Rauber, J.R. Klein, and M.W. Cole, Phys. Rev. B **27**, 1314 (1983).

[18] A.D. McLachlan, Mol. Phys. **7**, 381 (1964).

[19] G. Vidali, G. Ihm, H.-Y. Kim, and M.W. Cole, Surf. Sci. Rep. **12**, 135 (1991).

[20] L.W. Bruch, Surf. Sci. **125**, 194 (1983).

[21] R.D. Diehl and S.C. Fain, J. Chem. Phys. **77**, 5065 (1982).

[22] C.G. Shaw and S.C. Fain, Surf. Sci. **83**, 1 (1979).

[23] S.C. Fain and M.D. Chinn, J. Phys. **38**, C4 (1977).

[24] Jinhe Cui, Ph.D. thesis, University of Washington, 1988.

[25] S. Calisti, J. Suzanne, and J.A. Venables, Surf. Sci. **115**, 455 (1982).

[26] A.A. Antoniou, J. Chem. Phys. **64**, 4901 (1976).

[27] P.S. Schabes-Retchkiman and J.A. Venables, Surf. Sci. **105**, 536 (1981).

[28] J. Unguris, L.W. Bruch, E.R. Moog, and M.B. Webb, Surf. Sci. **109**, 522 (1981).

[29] G.S. Leatherman and R.D. Diehl, Langmuir **13**, 7063 (1997).

[30] J. Unguris, L.W. Bruch, E.R. Moog, and M.B. Webb, Surf. Sci. **87**, 415 (1979).